*China Steel Technical Report, No. 33, pp.24－35, (2020)*

# Characterization and Application of Chromium-free Galvannealed Steel Sheet

**CHING-KUO KUO* and GERALD S. FRANKEL****

** New Materials Research & Development Department, China Steel Corporation*
*** Fontana Corrosion Center, the Ohio State University, U.S.A*

**In response to the environmental issue, the post-treatment of galvanized steel is gradually moving toward a surface treatment without trivalent nor hexavalent chromium. In this study, the hot dip galvannealed steel sheet was used as the substrate to study the performance among chromium-free and commercial chromate samples. Surface characteristics, corrosion resistance and painting application were investigated by 3-dimension optical profiler, scanning electron microscope, atomic force microscope, and electrochemical methods. Results were summarized as follows: (1) From macroscopic to microscopic analyses, surface characteristics were clearly studied, and it was indicated that the overall roughness was affected by the surface texture of alloy layer and the thickness of conversion coating. (2) Polarization curve and Nyquist results showed that the chromium-free A sample had the lowest corrosion current (1.48 μA / $cm^2$) and the highest low-frequency impedance (7,261 Ω·$cm^2$), indicating that its corrosion resistance was better than that of other samples. (3) Cyclic corrosion test of painted samples showed that chromium-free samples met requirements. Besides, microstructure analysis confirmed that anodic undermining was the main cause of blistering or delamination. (4) Pull-off test and microstructural analysis showed that adhesion of chromium-free samples were better than that of chromate samples. It was because of the thin inorganic chromate coating was unable to enhance the interfacial bonding effectively.**

**Keywords: Galvannealed Steel, Chromium-Free Coating, Corrosion Resistance**

## 1. INTRODUCTION

The demand for zinc-coated steel sheet has risen dramatically in recent years due to the requirements of corrosion protection, forming ability, and welding ability in automotive manufacturing[1-2]. Moreover, Zn-Fe alloy coated steel (hot dip galvannealed steel; GA) with the higher melting point and the larger surface roughness has applied progressively in architecture application, e.g., roller shutter, fireproof door, painted cabinet.

Manufacturing process of hot dip galvannealed steel coil in the continuous galvanizing line[3] is as follows: First, cold rolled coils on the entry side are welded, surface cleaned and then annealed in furnaces. Then the strip coming out from the annealing furnaces, dips into the zinc pot and heats up again for Fe-Zn alloying. On the delivery side, strip pass though a skin pass mill and tension leveller. Finally, post-treatment is applied to the coils according to customer's request. In the stage of Fe-Zn alloying[4-5], iron atoms of the cold rolled substrate are diffused into the zinc layer during the heating section. Afterwards, the multi-phase Zn-Fe alloying layer is formed and accompanied with the irregular surface texture.

In response to the environmental issue of non-chromium construction materials[6] and related regulations restricting or canceling chromate surface treatment[7-8], China Steel Corporation (CSC) has begun to develop chromium-free passivated GA steel to replace the chromate GA product. In terms of corrosion resistance and painting application of chromium-free treated products, motivations in this study contained four parts, including: (1) Surface characterization of chromium-free samples, (2) Corrosion resistance of chromium-free samples, (3) Corrosion behavior of painted samples, and (4) Adhesion behavior of painted samples.

## 2. EXPERIMENTAL PROCEDURE

### *2.1 Experimental Methods*

In this study, specimens were made of GA steel produced by CSC. Thickness of specimens was controlled to 1.6 mm, and the alloy layer adopted F12, which was according to JIS standard[6]. Three post-treatments were collected as follows: chromium-free A treatment (Cr-free A), chromium-free B treatment (Cr-free B), and chromate treatment (Cr). Both chromium-free treatments adopted chromium-free chemicals developed from CSC's

R&D department, in which the coating thickness of Cr-free A was higher than that of Cr-free B, and Cr sample was the commercial chromate product of CSC.

The coating properties of the specimens, including corrosion resistance and painting ability, were evaluated. (1) Corrosion resistance: the percentage of the rust of the treated samples was measured by salt spray tests (ASTM B117) with 48-120 hours. (2) Painting ability: the treated samples were painted with a commercial acrylic paint, where the coating thickness was controlled to 30 μm. The painted samples were cured at a temperature of 220°C for 15 minutes. Afterwards, the painted samples were tested by the following methods. (i) Corrosion resistance: the painted samples were cut in "X" and exposed to the cyclic corrosion test (CCT；JASO M609-91) 45 times. After the test, if the width of the blister near the scratched region was smaller than 3 mm it passed the test. (ii) Pull-off adhesion: the painted samples were immersed in boiling water for 2 hours. Then paint delamination was assessed with the PosiTest ATA pull-off adhesion tester (ASTM D4541 / D7234).

### *2.2 Analyzing and Electrochemical Methods*

On the other hand, surface morphologies from macroscopic to microscopic analyses were observed by 3D optical profiler (OP), scanning electron microscope (SEM), and atomic force microscope (AFM), respectively. Cross-sectional morphology was manufactured and analyzed by focus ion beam (FIB) and energy dispersive spectrometer (EDS). Polarization curves of specimens were conducted in 3.5wt% $NaCl_{(aq)}$ solution and the testing area was around 0.8 $cm^2$ with the use of platinum mesh as the auxiliary electrode, and saturated calomel electrode (SCE) as the reference electrode. While the open circuit potential was to be stable, it started to scan from 500 mV below the open circuit potential toward the anode to 500 mV above the open circuit potential at a scan rate of 1 mV/s. Electrochemical impedance spectroscopy (EIS) measurements of specimens were performed by 3.5wt% $NaCl_{(aq)}$ solution and the testing area was around 5.0 $cm^2$ with the use of platinum mesh as the auxiliary electrode, and saturated SCE as the reference electrode. While the open circuit potential was to be stable, the frequency of the EIS test ranged from $10^5$ Hz to $10^{-2}$ Hz with 10 mV sine wave signal to the open circuit potential was applied and presented as a Nyquist plot.

## 3. RESULTS AND DISCUSSION

### *3.1 Surface characterization of chromium-free samples*

Surface morphologies of the materials were successfully investigated through OP, SEM, and AFM. Those techniques not only provide more realistic morphologies and quantitative roughness, but also help us understand the surface characteristic of each sample.

Fig.1 and Fig.2 show surface morphologies of the Cr-free A sample; Fig.3 and Fig.4 show surface morphologies of the Cr-free B sample; Fig.5 and Fig.6 show morphologies of the Cr sample. OP observed the depth difference of the surface under macroscopic view, but it was not easy to distinguish the coating from the alloy layer. SEM clearly showed the realistic texture, and partly observed the coverage of the coating. AFM exhibited differences in morphology and roughness in the microscopic area, and the appearance of the coating composition might be observed, too (e.g., tiny particles were observed in Fig.2 or Fig.4).

Results of the three samples show that the morphology of the alloy layer includes plateau-like peak areas and valley areas with crystalline structures[3]. Among them, since the thickness of chromate coating was only around 0.1 - 0.2 um, its morphology was close to that of untreated alloy layer. In addition, compared with the morphology of the Cr-free B sample, coverage of the Cr-free A sample in the valley area was significantly better than that of the Cr-free B sample. This is ascribed that the solution was squeezed to the valley area by the roller during post-treatment. That's the main reason why Cr-free A sample has better coverage in the valley area.

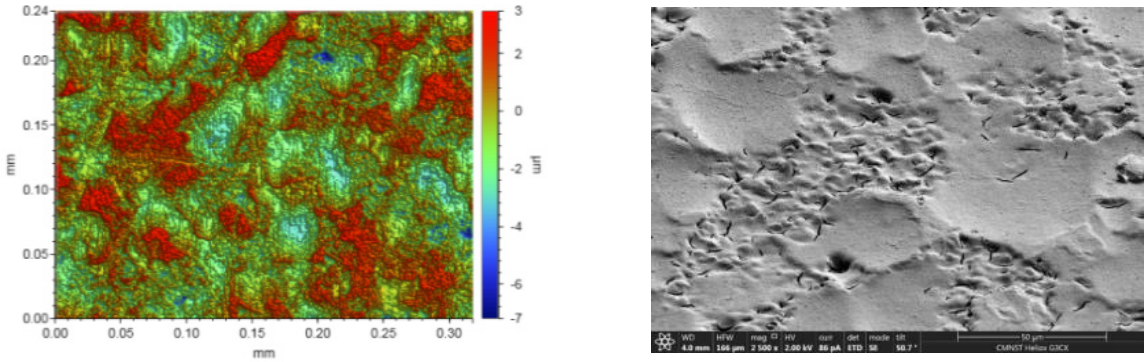


(a) (b)

**Fig.1.** Surface morphology of Cr-free A sample. (a) OP; (b) SEM

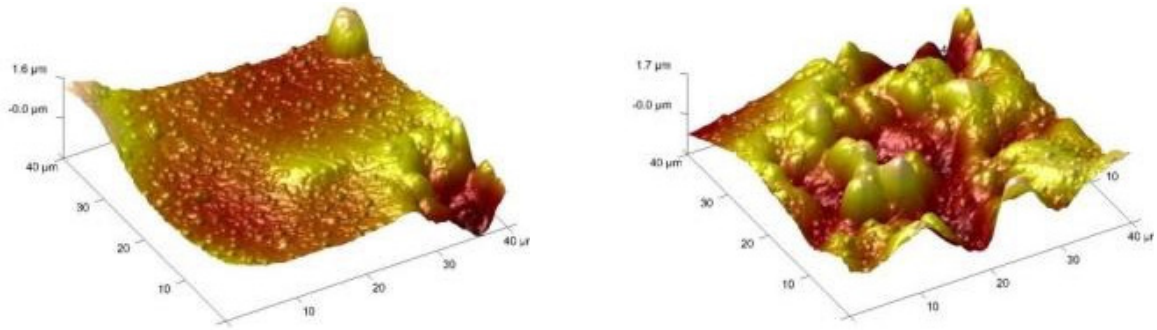

(a) (b)

**Fig.2.** Surface morphology of Cr-free A sample by AFM. (a) peak area; (b) valley area

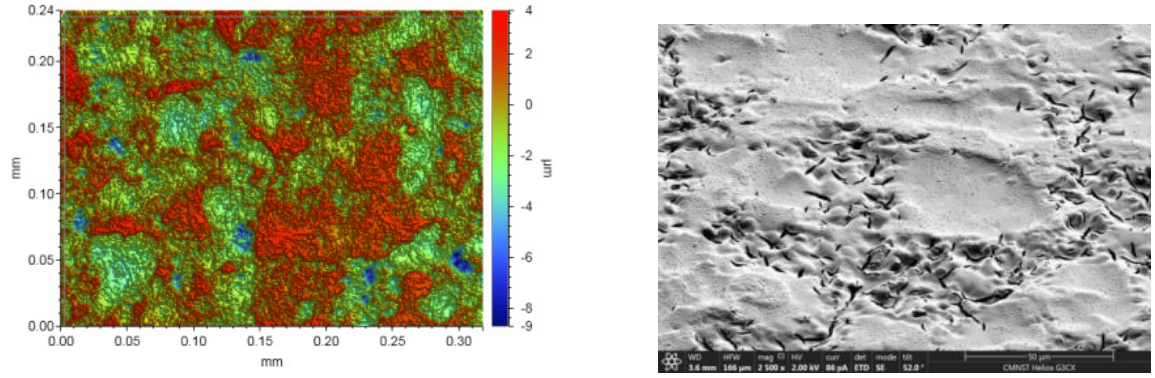

(a) (b)

**Fig.3.** Surface morphology of Cr-free B sample. (a) OP; (b) SEM

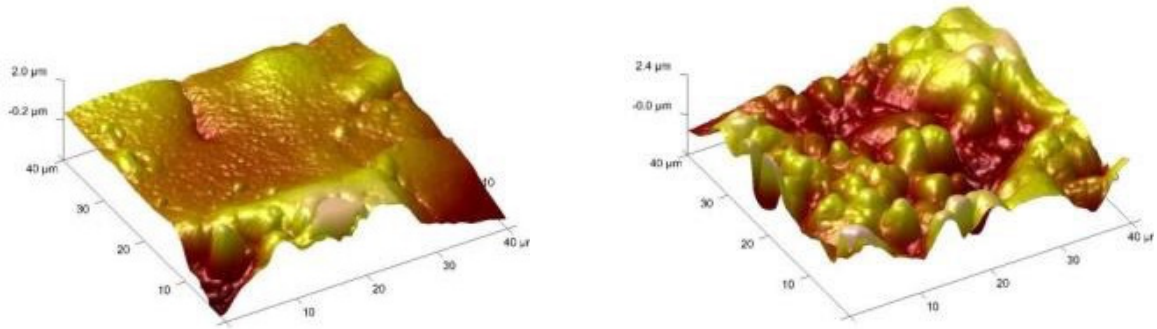

(a) (b)

**Fig.4.** Surface morphology of Cr-free B sample by AFM. (a) peak area; (b) valley area

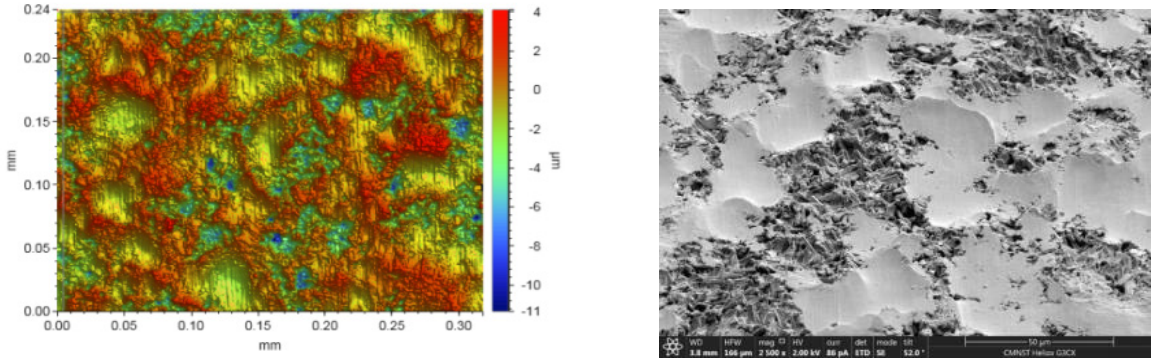

(a) (b)

**Fig.5.** Surface morphology of Cr sample. (a) OP; (b) SEM

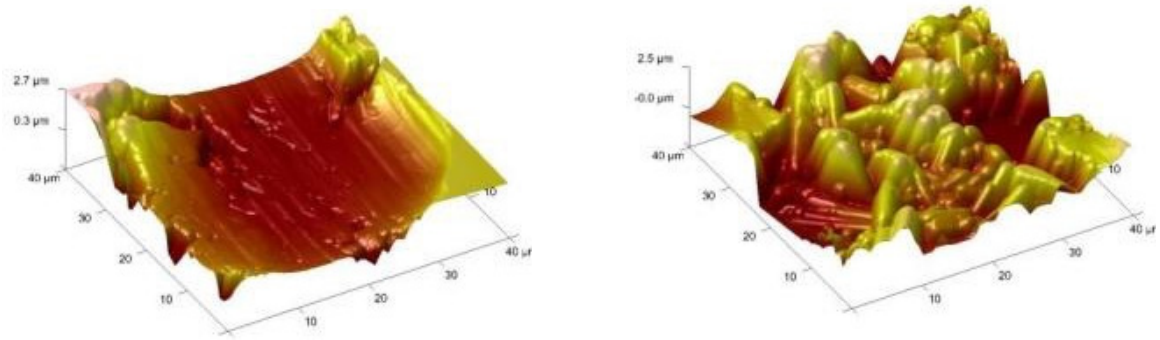

(a) (b)

**Fig.6.** Surface morphology of Cr sample by AFM. (a) peak area; (b) valley area

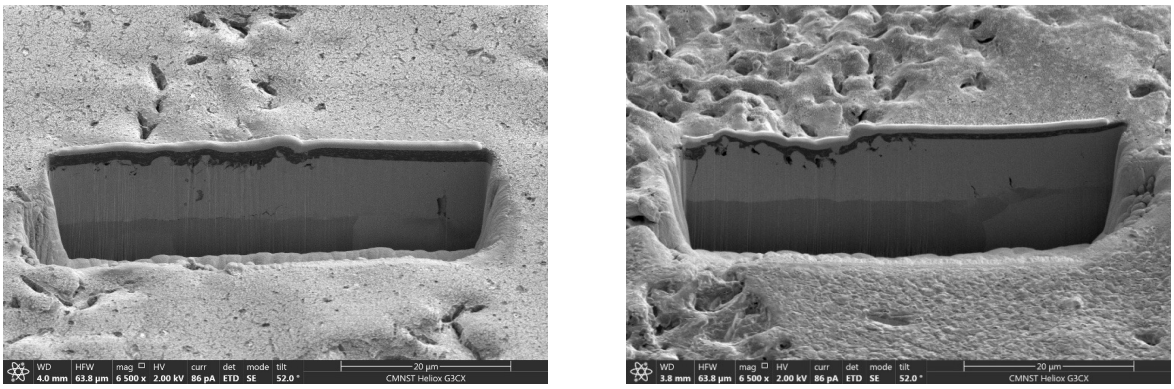

(a) (b)

**Fig.7.** Cross sectional morphologies of Cr-free samples. (a) Cr-free A; (b) Cr-free B

On the other hand, the cross-sectional morphologies of the Cr-free samples were observed by FIB and SEM, as shown in Fig.7. The black area in the image was the Cr-free coating, and the alloy layer was under the coating. In Fig.7, it confirmed that Cr-free A sample almost completely covered the alloy layer, especially in the valley area, due to the higher coating thickness, while Cr-free B sample did not completely cover the alloy layer because its thickness was insufficient.

In addition, Fig.8 collated the roughness data measured by OP for each sample. The results can be summarized as follows: (1) Due to the influence of the roll coating, $R_z$ (10-point high-low average roughness) and $R_v$ (maximum profile valley depth) of chromium-free samples decreased with increasing the coating thickness, and $R_p$ (maximum profile peak height) was less affected by the coating thickness. (2) Since thickness of the chromate coating was extremely thin, the roughness and morphology were approximate to those of the untreated alloy layer.

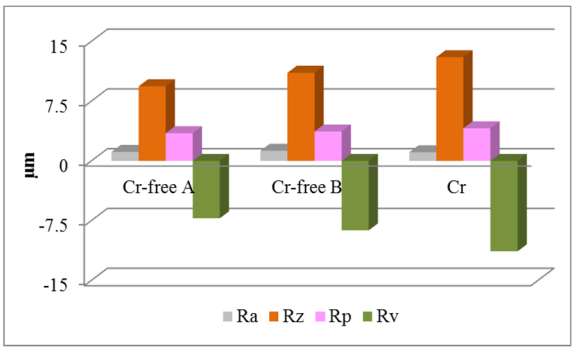


**Fig.8.** Roughness of each sample by OP.

### *3.2 Corrosion resistance of chromium-free samples*

Fig.9 shows the electrochemical results of each sample under 3.5wt% $NaCl_{(aq)}$ solution. Polarization curves (Fig.9(a)) and the corrosion current ($I_{corr}$) in Table 1 showed that $I_{corr}$ of the untreated GA sample was 9.33 μA/cm$^2$, which was the highest among all samples, indicating the worst corrosion resistance. Though $I_{corr}$ of other treated samples looked close, $I_{corr}$ of the Cr-free A sample (1.48 μA /cm$^2$) was still the lowest, indicating the best corrosion resistance. Nyquist plot in Fig.9(b) and impedance in Table 1 also showed that the untreated GA sample had the lowest impedance value, indicating that

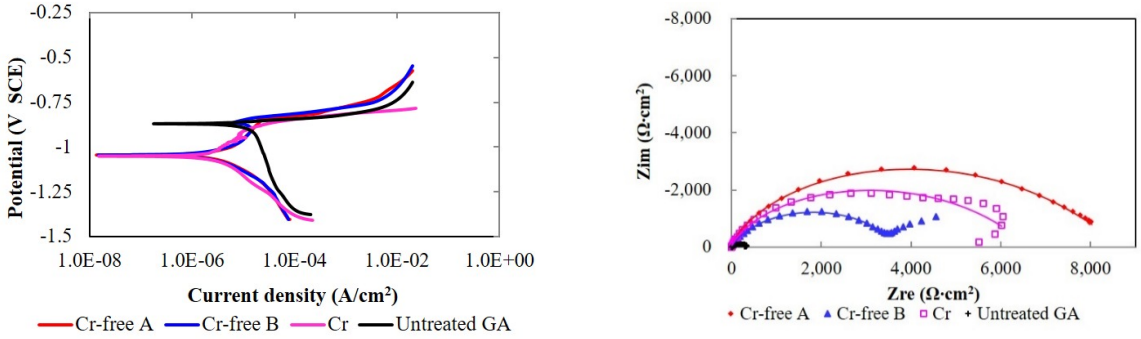


(a) (b)

**Fig.9.** Electrochemical results of each sample. (a) Polarization curves; (b) Nyquist plots

**Table 1** Corrosion current and Impedance of each sample under 3.5wt%NaCl(aq).

| Samples | Cr-free A | Cr-free B | Cr | Untreated GA |
|---|---|---|---|---|
| $I_{corr}$ (μA /cm$^2$) | 1.48 | 1.68 | 2.14 | 9.33 |
| Impedance (Ω·cm$^2$) | 7,261 | 3,682 | 6,626 | 268 |

its corrosion resistance was also the worst. The low-frequency impedance of other treated samples was in order: Cr-free A (7,261 Ω·cm$^2$) > Cr (6,626 Ω·cm$^2$) > Cr-free B (3,682 Ω·cm$^2$). Both electrochemical results were approximately the same as the salt spray results in Fig.10, confirming that the newly developed Cr-free A sample has the best corrosion resistance. In addition, compared with the Cr-free A sample, the impedance of the Cr-free B sample was significantly lower, and it appeared a tail-like diffusion behavior at the low-frequency impedance, indicating that it is easy to accelerate corrosion of the alloy layer while the coating coverage was insufficient.

### *3.3 Corrosion behavior of painted samples*

3.3.1 Corrosion test of painted samples

In order to investigate corrosion resistance of samples after painting, CCT was carried out for 45 cycles. Afterward samples were taken out for evaluation and microscopic analysis.

Fig.11 shows the results of 45 cycles of corrosion test for Cr-free A, Cr-free B, and Cr painted samples. The measured blister width of each sample was ≤ 3 mm, which confirmed that all CSC's products met the requirements.

**Fig.10.** Salt spray test with 120 hours of each sample. (a) Cr-free A; (b) Cr-free B; (c) Cr

3.3.2 Microstructural analysis on the scratched area of painted samples

In order to study the corrosion behavior of painted samples in the cyclic corrosion test, microstructures of the corrosion area of two samples were analyzed.

(a) Cr-free A painted sample

Fig.12(a) shows the top view image of the Cr-free A painted sample near the scratched area, and Table 2 performs EDS analysis on specific areas. Comparing the results of Fig.12(a) and Table 2, it can be concluded that: 1. Area (a) belongs to the top coat. 2. Area (b) contained the alloy layer, the coating, and zinc corrosives and/or chloride derivatives; 3. Area (c) covered zinc and iron corrosives near the scratched area; 4. Area (d) was a cold-rolled substrate without the alloy layer.

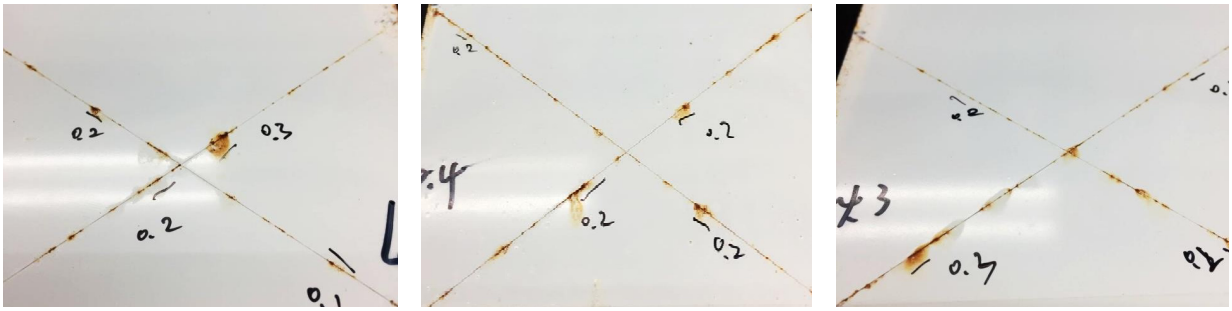

(a) (b) (c)

**Fig.11**. Test results of the 45th cyclic corrosion test. (a) Cr-free A; (b) Cr-free B; (c) Cr

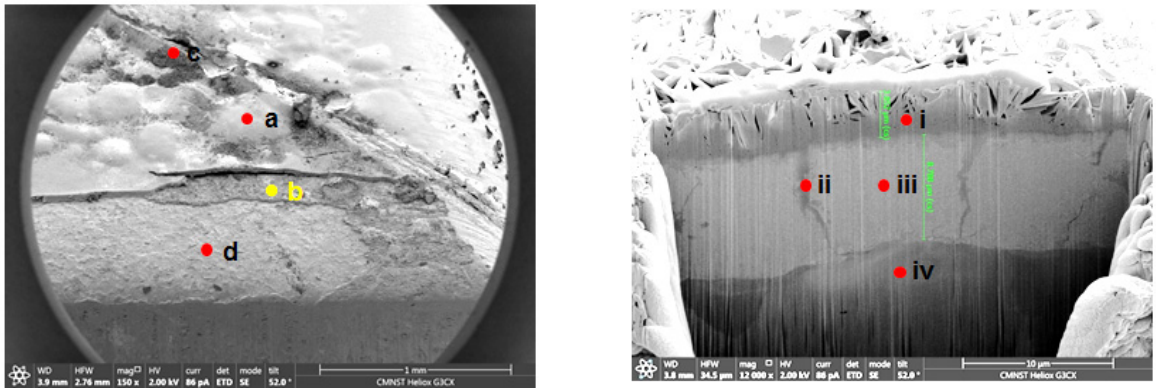


(a) (b)

**Fig.12.** Morphologies of Cr-free A painted sample after CCT. (a) top view; (b) cross section

**Table 2** EDS results of Cr-free A painted sample after CCT

| | a | b | c | d |
|---|---|---|---|---|
| C | 34.3 | 19.2 | 5.9 | 3.9 |
| O | 25.8 | 12.2 | 20.0 | 1.3 |
| Na | 0.4 | 1.2 | 2.1 | - |
| Al | 0.6 | - | - | - |
| Si、Zr | - | 5.2 | - | - |
| Cl | - | 12.3 | 6.3 | 0.6 (F) |
| Ti | 35.5 | - | 1.6 | - |
| Fe | 1.5 | 2.5 | 33.3 | 88.1 |
| Zn | 1.9 | 47.4 | 30.7 | 6.1 |
| Total | 100.00 | 100.00 | 100.00 | 100.00 |
| Remarks | Painted layer | Alloy layer, $Zn(OH)_2$, Coating | $Zn(OH)_2$, $Fe_xO_y$ | Substrate |

On the other hand, the cross-sectional analysis was performed for area (b), as shown in Fig.12(b). Table 3 shows the EDS results from (i) - (iv) regions. Region (i) showed the distribution of Cl and O elements on the surface of the alloy layer, expressed as zinc corrosives ($Zn_x(OH)_yCl_z$)[9]. In addition, the result of region (ii) was similar to that of region (i), indicating that chloride ions can penetrate into the alloy layer and cause anodic attack or anodic undermining[10-11]. Region (iii) maintained the original distribution of the alloy layer, indicating that this area had not been corroded. Finally, region (iv) belonged to a cold-rolled substrate.

(b) Cr painted sample

Fig.13(a) shows the top view image of the Cr painted sample near the scratched area, and Table 4 performs EDS analysis on specific areas. Comparing the results of Fig.13(a) and Table 4, the results can be summarized: 1. Area (a) was the top coat. 2. Area (b) covered the zinc corrosives and/or chloride derivatives. 3. Area (c) contained the alloy layer, and zinc corrosives and/or chloride derivatives. 4. Area (d) contained the alloy layer, zinc corrosives and/or chloride derivatives, and iron corrosives. 5. Area (e) was the cold-rolled substrate without the alloy layer.

In addition, surface and cross-sectional morphologies of area (c) were also analyzed by Fig.13(b). Fig.13(b) showed that the surface of the alloy layer was covered with a large amount of zinc corrosives, and the cross section showed that a large amount of chloride ions gradually penetrate into the layer from the outside to form a basic zinc chloride corrosives [9], similar to the corrosion process in Fig.13. Those are also the main reasons for the blistering or delamination of the painted layer.

3.3.3 Corrosion mechanism on the scratched area of the painted samples

In general, delamination or blistering of the painted layer comes from cathodic delamination, anodic undermining, etc.[10-11]. This study by microstructure analysis confirmed that the corrosion behavior of these series of painted samples after cyclic corrosion test seemed to be similar, and was mainly based on anodic undermining. Therefore, a schematic diagram of corrosion near the scratched area was shown in Fig.14. The anodic and cathodic reactions are summarized in Eq. (1) ~ Eq. (7)[9],

**Table 3** EDS results of cross section of spot b of **Cr-free A p**ainted sample.

| | i | ii | iii | iv |
|---|---|---|---|---|
| C | 2.05 | 1.83 | 1.39 | 0.64 |
| O | 10.32 | 6.76 | 0.51 | - |
| Cl | 14.40 | 7.34 | - | - |
| Fe | 12.61 | 27.43 | 28.23 | 98.40 |
| Zn | 60.62 | 56.65 | 69.87 | 0.96 |
| Total | 100.00 | 100.00 | 100.00 | 100.00 |
| Remarks | $Zn(OH)_2$ | $Zn(OH)_2$ | Alloy layer | Substrate |

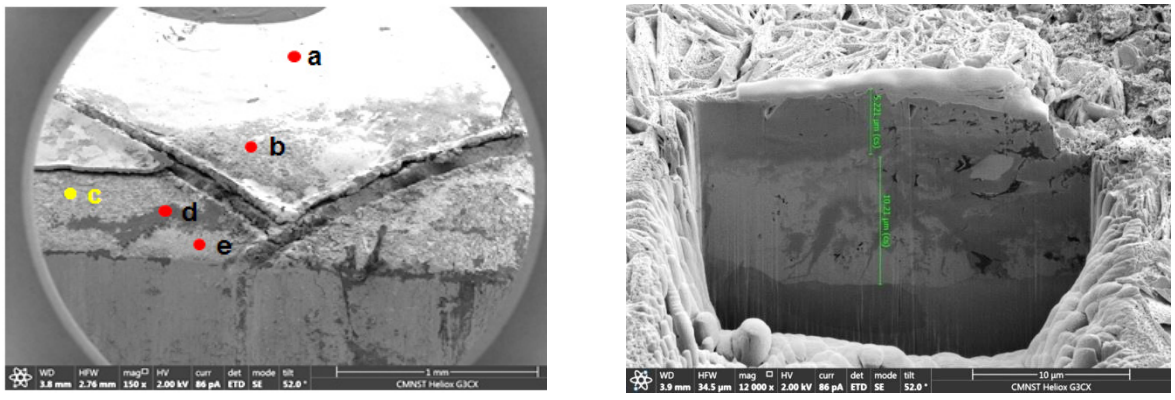


(a) (b)

**Fig.13.** Morphologies of Cr painted sample after CCT. (a) top view; (b) cross section

**Table 4** EDS results of Cr painted sample after CCT

| | a | b | c | d | e |
|---|---|---|---|---|---|
| C | 40.82 | 10.74 | 6.11 | 2.75 | 2.70 |
| O | 24.72 | 25.84 | 16.18 | 16.09 | - |
| Na | - | 3.04 | 1.25 | - | - |
| Al | 0.57 | - | - | - | - |
| S | - | 0.48 | - | - | - |
| Cl | - | 1.01 | 13.09 | 14.09 | 0.20 |
| Ti | 32.76 | 1.53 | 0.61 | - | - |
| Fe | 0.72 | 4.13 | 3.08 | 13.32 | 97.10 |
| Zn | 0.41 | 53.23 | 59.68 | 53.74 | - |
| Total | 100.00 | 100.00 | 100.00 | 100.00 | 100.00 |
| Remarks | Painted layer | $Zn(OH)_2$ | Alloy layer, $Zn(OH)_2$ | $Zn(OH)_2$, $Fe_xO_y$ | Substrate |

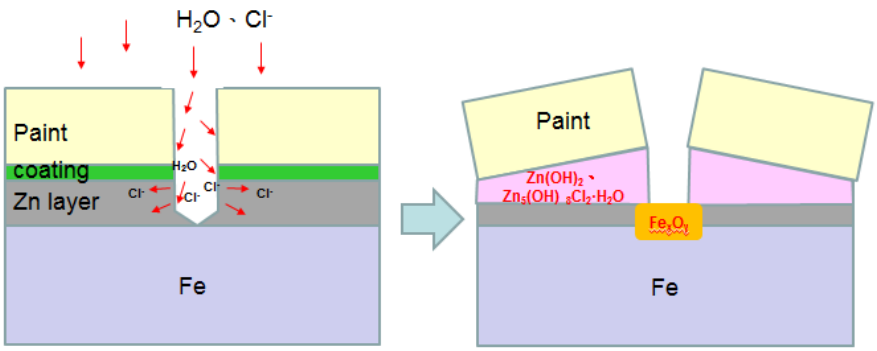


**Fig.14.** Illustration of corrosion process on the scratched area of painted sample

in which the anode contains the oxidation or corrosion reactions of the zinc from the alloy layer and the iron from the substrate.

Cathodic reaction：$O_2 + 2H_2O + 4e \rightarrow 4OH^-$.... (1)

Anodic reactions：

$Zn \rightarrow Zn^{2+} + 2e$..... (2)

$Zn + 2H_2O \rightarrow Zn(OH)_2 + 2H^+ + 2e$ ..... (3)

$5Zn^{2+} + 2Cl^- + 8OH^- + H_2O \rightarrow$

$Zn_5(OH)_8Cl_2{\cdot}H_2O$ ..... (4)

$Fe \rightarrow Fe^{2+} + 2e$ ..... (5)

$Fe^{2+} + 2OH^- \rightarrow Fe(OH)_2$ ..... (6)

$2Fe(OH)_2 + 1/2\ O_2 + H_2O \rightarrow$

$2Fe(OH)_3\ Fe(OH)_3 \rightarrow FeOOH + H_2O$ ..... (7)

Overall, the corrosion process is presumed to be: corrosion factors ($Cl^-$) easily penetrated into the painted layer, the alloy layer or the substrate made metal corrode from the scratched area. Finally, corrosion products resulted in blister or delamination. That's one of the reasons why adhesion usually deteriorates after corrosion.

In summary, the main factors affecting the corrosion resistance of painted samples include paints, thickness, and the painted layer. The quality of painting determines the corrosion rate. Although the coating can slow down the formation of corrosion products in the alloy layer, the test results showed that this effect was not as obvious as the painted layer. From those results, it is known that the corrosion resistance of the chromate and Cr-free products of CSC meets the application requirements.

### *3.4 Adhesion behavior of painted samples*

3.4.1 Adhesion results of painted samples

Fig.15 shows adhesion results of Cr-free A, Cr-free

B and Cr painted samples. According to the cross hatch test, no painted layer peeled off from those samples, and difference could not be compared. On the other hand, from the pull off test, the results of the Cr-free A sample showed only slight peeling. The peeling area of the Cr-free B sample was slightly more serious than that of the Cr-free A sample. However, the peeling area of the Cr sample was the most serious, indicating that the adhesion of the Cr sample was the worst, and the adhesion of each sample can be clearly distinguished by pull-out test. In addition, microstructure analysis was performed on specific areas after testing to discuss each difference.

3.4.2 Microstructural analysis on the pull-off area of painted samples

Cr-free A painted sample

First, regarding the cross-sectional analysis of the Cr-free A painted sample, Fig.16 observed that the surface of the Cr-free A painted sample was covered with residual glue, which belonged to glue failure. Since the thickness of the painted layer was around 30 μm, the total thickness of the black area measured in Fig.16(a) reached 45 μm, so it can be determined that the upper part came from the residual glue. Fig.16(b) showed the interface between the painted layer and the alloy layer. It was also demonstrated that the interface area adhered a coating with a thickness ranging from 1.0 to 2.0 μm. The cross-sectional results confirmed that the painted layer, the coating, and the alloy layer were closely adhered and had good adhesion.

Cr-free B painted sample

The SEM image shown in Fig.17 also observed that the surface of the Cr-free B painted sample was covered with residual glue, which also belonged to glue failure. Fig.17(a) measured the total thickness to be around 45 μm, so it also confirmed that the upper part came from the residual glue. Fig.17(b) showed the interface between the painted layer and the alloy layer. It was also demonstrated that the interface area adhered a coating with a

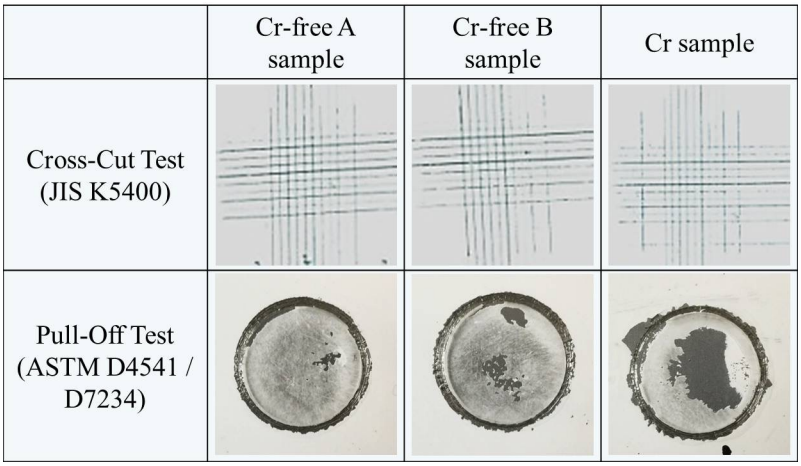


**Fig.15.** Results of adhesion test for each painted sample

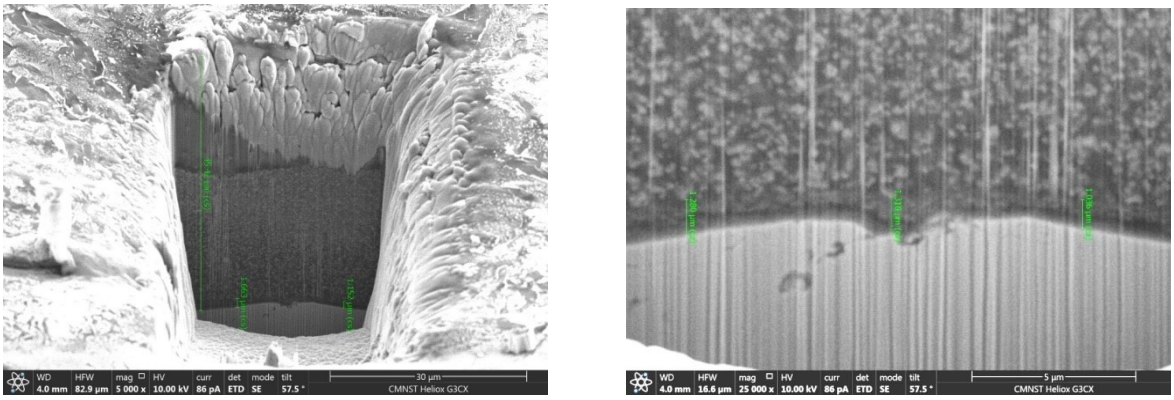

(a) (b)

**Fig.16.** Cross sectional morphologies of Cr-free A painted sample. (a) 5,000x; (b) 25,000x

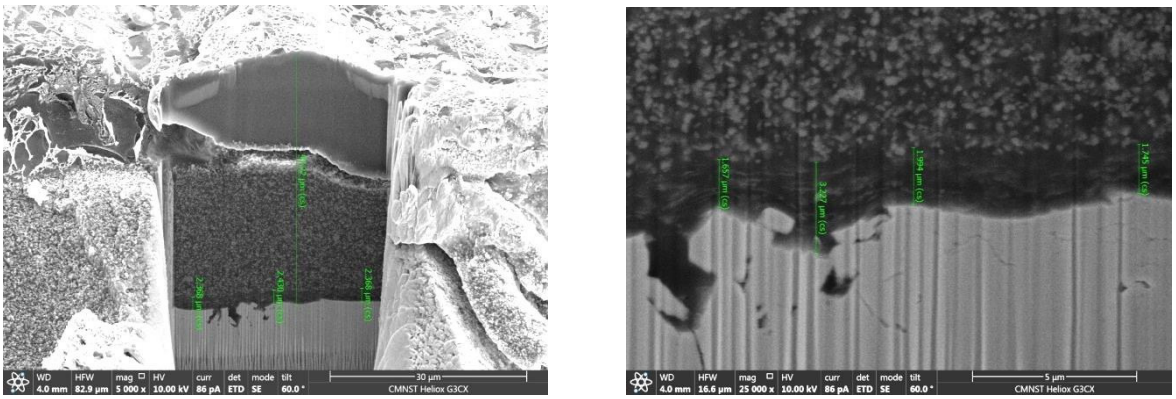

(a) (b)

**Fig.17.** Cross sectional morphologies of Cr-free B painted samples. (a) 5,000x; (b) 25,000x

thickness ranging from 1.0 to 2.0 μm. The cross-sectional results confirmed that the painted layer, the coating, and the alloy layer were closely adhered and have good adhesion.

On the other hand, the slightly peeling areas of the Cr-free B painted samples were also analyzed by SEM, as shown in Fig.18. EDS analysis was performed on areas 1 to 3 in Fig.18, and the results were shown in Table 5. It showed that the peeling regions of area 1 and area 2 still contain Zr and Si elements which belonged to coating compositions, whereas the incomplete peeling region (area 3) contained Ti element which came from $TiO_2$ pigment of the painted layer. The results showed that the painted layer in the peeling area was an adhesive fracture, but the adhesion between the coating and the alloy layer remained good, which confirmed that the adhesion between the coating and the alloy layer was better than that between the painted layer and the coating. It is also indicated that the adhesion may be mainly affected by the painted layer.

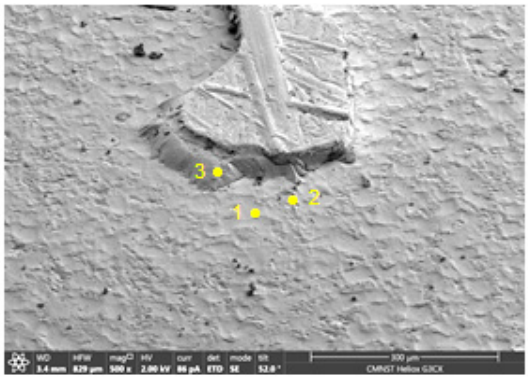


**Fig.18.** Surface morphology of the peeling area of Cr-free B painted sample.

**Table 5** EDS results of the peeling area of Cr-free B painted sample

| | 1 | 2 | 3 |
|---|---|---|---|
| C | 61.36 | 47.93 | 31.28 |
| O | 15.77 | 11.42 | 26.57 |
| Al | - | 0.24 | 0.83 |
| Si, Zr | 6.30 | 13.82 | |
| Ti | 0.68 | 0.82 | 40.29 |
| Fe | 1.41 | 1.75 | 0.88 |
| Zn | 14.47 | 24.02 | 0.15 |
| Total | 100.00 | 100.00 | 100.00 |
| Remarks | Coating | Coating | Painted layer |

Cr painted sample

The SEM image also observed that the surface of the unpeeling area of the Cr painted sample was covered with residual glue, which was a glue failure. Cross section in Fig.19(a) showed that the peeling area included the results of both adhesive and cohesive fracture. Fig.19(b) showed that the adhesive fracture was distributed in the peak area of the alloy layer, and the cohesive fracture was distributed in the valley area with the higher roughness of the alloy layer. It means that the mechanical interaction on the high roughness area enhanced the adhesion and resulted in the cohesive fracture.

3.4.3 Comparison of Adhesion of painted samples

The adhesion and microstructural results of the three samples are summarized in Table 6. It can be summarized as follows: (1) The adhesion was in order: Cr-free A sample > Cr -free B sample > Cr sample. (2) The worst adhesion of the Cr sample is ascribed that the inorganic chromate coating with the extremely thin thickness, which did not improve the interfacial bonding. Its adhesion only depended on the mechanical bonding between the painted layer and the roughness of the alloy layer. (3) Regarding the peeling area of the Cr-free samples, the coating was still tightly attached to the alloy layer, confirming that the adhesion of the coating and the alloy layer was better than the adhesion of the painted layer and the coating. It is also indicated that the adhesion may be mainly affected by the painted layer.

## 4. CONCLUSIONS

(1) The surface topographies of GA steel with post-treatment were investigated, and the characteristics and roughness of the surface were clearly understood from macroscopic to microscopic analyses. It was confirmed that the alloy layer covered the plateau-like peak area and the valley area with uneven crystalline structures. Among them, the overall roughness was affected by the alloy layer and the coating thickness, which can be summarized as: (i) Due to the roll coating process, $R_z$ and $R_v$ of the chromium-free samples decreased with increasing coating thickness, but $R_p$ seemed not to be affected by the thickness. (ii) The roughness and morphology of Cr sample looked similar to that of the alloy layer because the thickness of the chromate coating was extremely thin.

(2) Electrochemical results showed that the corrosion current of the Cr-free A sample was the lowest (1.48 μA /cm$^2$). The Nyquist plots also showed the low-frequency impedance of the Cr-free A sample Up to 7,261 Ω·cm$^2$, which was higher than other samples. Both results were consistent with the salt spray results, confirming that the newly developed chromium-free sample provide good corrosion resistance.

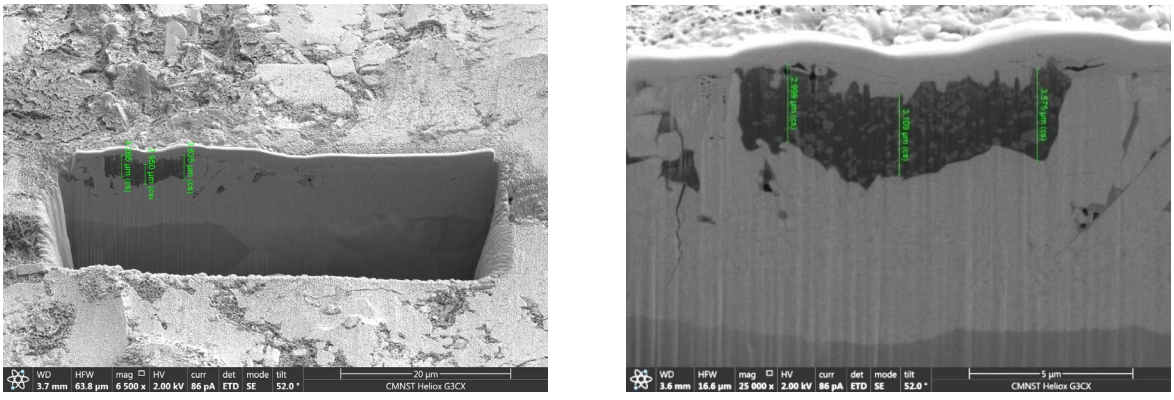


(a) (b)

**Fig.19.** Cross sectional morphologies of Cr painted sample. (a) 6,500x; (b) 25,000x

**Table 6** Comparison of each painted sample after pull-off test

| | Cr-free A | Cr-free B | Cr |
|---|---|---|---|
| Macro- | No peeling | Slight Peeling | Serious Peeling |
| Micro- | Glue failure on unpeeling area. | Glue failure on unpeeling area.<br>Adhesive fracture on peeling area. | Both adhesive and cohesive fractures on peeling area.<br>Residual paint on valley area. |

(3) Results of cyclic corrosion test of painted samples showed that the width of the blister for each sample was ≤ 3 mm, which made sure that all CSC's products met the requirements. Besides, microstructure analysis confirmed that anodic undermining was the main cause of blistering or delamination.
(4) Pull-off test and microstructural analysis showed that adhesion of chromium-free samples was better than that of the chromate sample. It was because of the thin inorganic chromate coating was unable to enhance the interfacial bonding effectively. Besides, microstructural analysis also confirmed that the adhesion between the Cr-free coating and the alloy layer was better than that between the painted layer and the Cr-free coating. It was also indicated that the adhesion may be mainly affected by the painted layer.
(5) This study completed the research on the surface characteristics, corrosion resistance, and painting application of Cr-free galvannealed steel sheets. It is confirmed that the performance of Cr-free samples is better than that of the chromate sample, and also meets customer requirements.

## REFERENCES

1. A. R. Marder: Prog. Mater. Sci., 2000, 45, p. 191.
2. S. D. Bakshi, M. Dutta, and D. Bhattacharjee: ISIJ International, 2005, 45 (9), p. 1368.
3. C. K. Kuo: Journal of Chinese Corrosion Engineering, 2015, 29(2), p. 81.
4. J. Mahieu, S. Claessens, and B. C. De Cooman: Metall. Mater. Trans. A, 2001, 32A, p. 2905.
5. S. Feliu and M.L. Perez-Revenga: Acta Mater., 2005, 53, p. 2857.
6. JIS G 3302 Standards. (Hot dip zinc coated steel sheets and coils)
7. The RoHS Directive. ( https://ec.europa.eu/environment/waste/rohs_eee/index_en.htm)
8. Safety and Health Topics / Hexavalent Chromium. (https://www.osha.gov/SLTC/ hexavalentchromium/)
9. L. J. Feng, P. F. Dong, Z. C. Cheng, L. Liu, C. F. Dong, X. G. Li, and K. Xiao, Surf. Tech., 2017, 46(8), p. 246.
10. Denny A. Jones: Principles and prevention of corrosion, 2nd ed., Macmillan book Co., New York, NY, 1992, p. 116.
11. S. T. Shen: Journal of Chinese Corrosion Engineering, 1993, 7(2), p. 1. □